quaternary

MDPI

Article

Seismic Activity in the Celje Basin (Slovenia) in Roman Times—Archaeoseismological Evidence from Celeia

Miklós Kázmér [1,*], Petra Jamšek Rupnik [2] and Krzysztof Gaidzik [3]

[1] MTA-ELTE Geological, Geophysical and Space Science Research Group, Department of Palaeontology, Eötvös University, 1117 Budapest, Hungary
[2] Geological Survey of Slovenia, SI-1000 Ljubljana, Slovenia
[3] Institute of Earth Sciences, University of Silesia in Katowice, 41-200 Sosnowiec, Poland
* Correspondence: mkazmer@gmail.com

Abstract: Searching for unknown earthquakes in Slovenia in the first millennium, we performed archaeoseismological analysis of Roman settlements. The *Mesto pod mestom* museum in Celje exhibits a paved Roman road, which suffered severe deformation. Built on fine gravel and sand from the Savinja River, the road displays a bulge and trench, pop-up structures, and pavement slabs tilted up to 40°. The city wall was built over the deformed road in Late Roman times, supported by a foundation containing recycled material (*spolia*) from public buildings, including an emperor's statue. We hypothesize that a severe earthquake hit the town before 350 AD, causing widespread destruction. Seismic-induced liquefaction caused differential subsidence, deforming the road. One of the nearby faults from the strike-slip Periadriatic fault system was the seismic source of this event.

Keywords: paleoseismology; Periadriatic fault system; active tectonics; Southern Alps; Pannonian Basin; Dinarides

check for updates

Citation: Kázmér, M.; Jamšek Rupnik, P.; Gaidzik, K. Seismic Activity in the Celje Basin (Slovenia) in Roman Times—Archaeoseismological Evidence from Celeia. *Quaternary* **2023**, *6*, 10. https://doi.org/10.3390/quat6010010

Academic Editors: Steven L. Forman and Marcello Tropeano

Received: 3 April 2022
Revised: 12 November 2022
Accepted: 28 January 2023
Published: 1 February 2023

1. Introduction

Slovenia is the seismically most active region of the Alpine–Dinaric junction. Several active faults have been recognized and mapped [1], presenting seismic hazard for the region [2]. The historical seismic catalogue of Slovenia [3] contains a multitude of data, but—inherently—mostly lacks any information for the first millennium. In this effect it shares its incompleteness with the catalogues of the neighbouring countries [4,5]. Therefore, further methods, such as palaeoseismology and archaeoseismology, are needed to find information at least on the strongest events in Slovenia [6]. We applied the methods of archaeoseismology [7–10] to find evidence for past earthquakes recorded by the built environment. We conducted a systematic survey of Roman settlements, inhabited mostly in the first to fourth centuries, to identify and parametrize unknown earthquakes in the Carpathian–Pannonian region [11]. Remnants of Roman architecture are eminently suitable for preserving evidence of past earthquakes [12]. In the absence of upright walls, collapse features and floor-level deformation additionally give evidence within the Pannonian Basin: Carnuntum in Austria [13], Brigetio in Hungary [14], Siscia in Croatia [15], Virunum (Magdalensberg) in Austria [16], to name a few. Celeia (modern Celje), the best-studied Roman town in Slovenia, displaying certain features which can be attributed to seismic damage, is the topic of the present paper.

1.1. Geological Background—Celeia

Celeia developed in the Celje Basin, located in NE Slovenia, at the transition from the Southern Alps to the Pannonian Basin system and in the eastern part of the Periadriatic fault system (Figures 1 and 2). The basin coincides with the post-Miocene Celje syncline [17,18], which according to Placer [19], belongs to the Sava folds structural domain. This is an asymmetrical syncline with a W–E oriented axis and a steeper southern limb [18]. The

basin lies between active faults, the Sava and Celje faults to the south and the Šoštanj fault to the north, which are part of the dextral–transpressive Periadriatic fault system [1,20,21]. The basin could be deformed transtensionally [20,22]. The Sava fault is an active dextral strike-slip fault with an estimated slip rate of 0.5–1.5 mm/year and a seismogenic potential of up to magnitude 6.8 [23,24] or even higher in case of activation of several segments [1]. In the western part in NE Italy and NW Slovenia, this fault is one of the possible sources of the 1348 M_w 6.4–7.0, I_{max} IX–X Carinthia earthquake [25–27]. The Šoštanj fault is an active dextral strike-slip fault with an estimated slip rate of 0.1–0.9 mm/year and a seismogenic potential of up to magnitude 7.0 when individual segments are activated [1]. In the eastern part of the Celje Basin, where Celeia is located, there are only 8 km between these two major active faults. The largest historical earthquake recorded in the immediate vicinity of the Celje Basin is the 1974 Mw 4.8, I_{max} VII Kozjansko earthquake [25]. The epicenter of this earthquake was located in the eastern part of the Sava folds, just SE of the Celje Basin and the Sava–Celje fault, but its source is unknown.

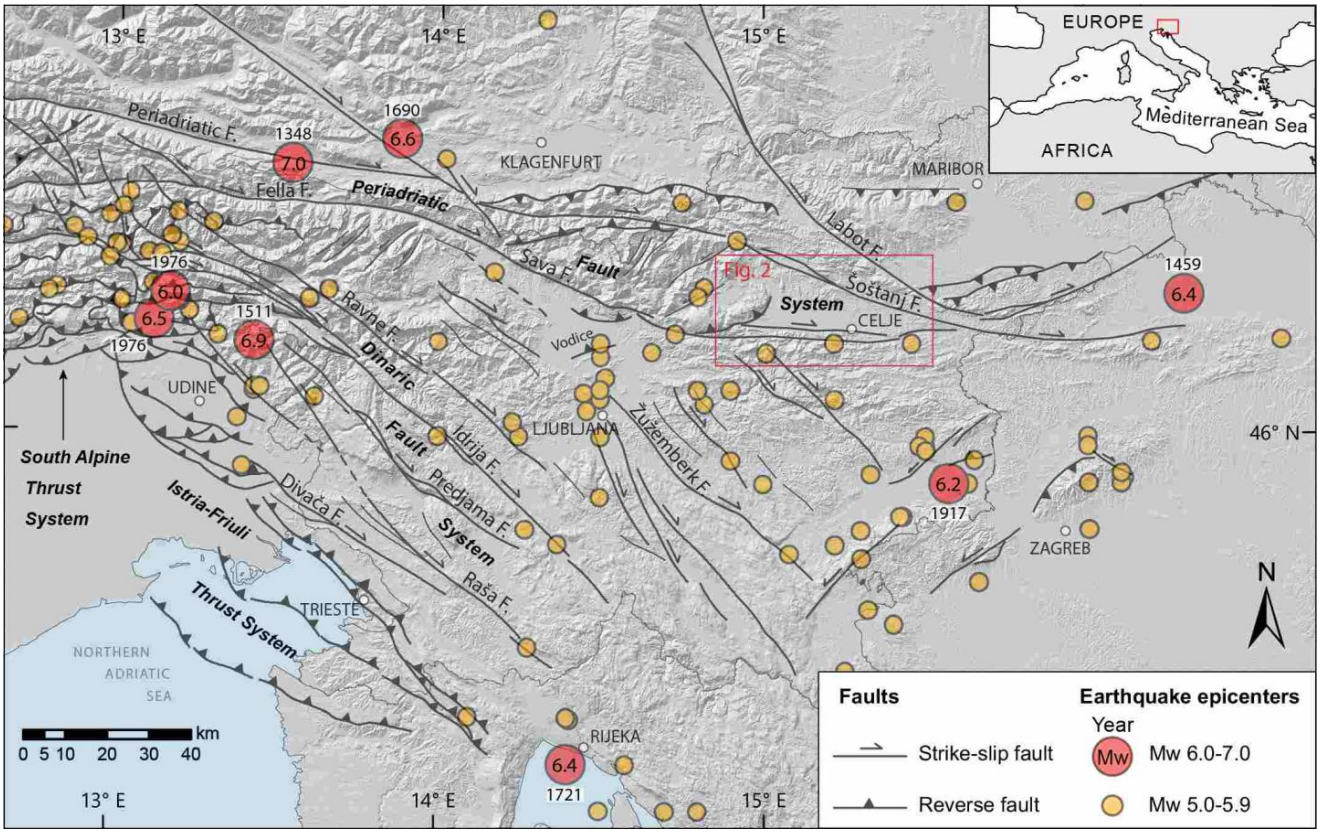

Figure 1. Active faults and seismicity of Slovenia (Mw $\geq$ 5.0). Note that along the Sava fault near Celje only Mw 5.0–5.9 earthquakes are known; the magnitude estimation, however, differs between the catalogues (see Figure 2 for comparison with Slovenian catalogue). The faults are summarized from [1,28], and the earthquakes are taken from the SHEEC catalogues 1000–1899 [29] and 1900–2006 [30].

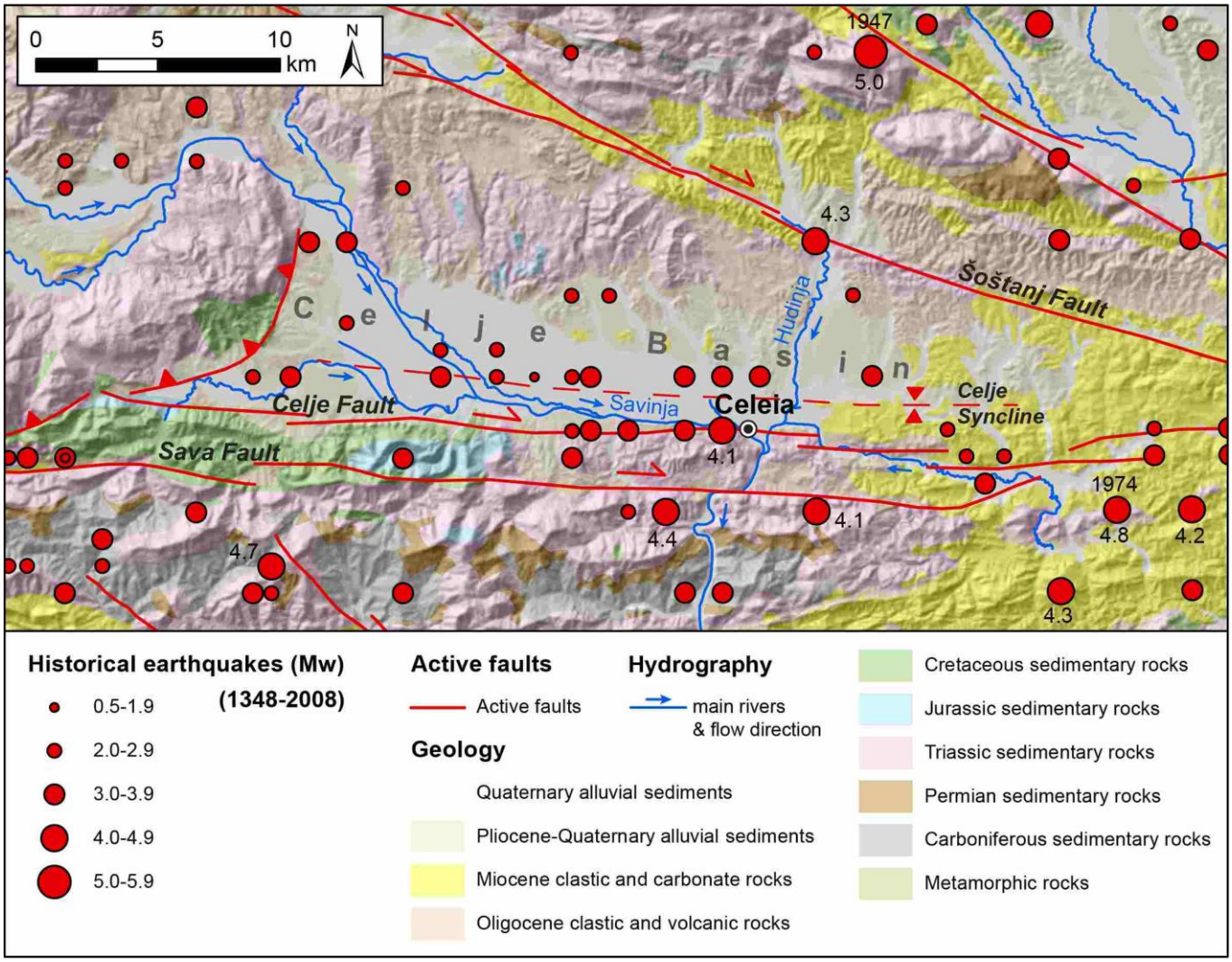

Figure 2. Geological setting of the Celje Basin with simplified geological units (redrawn after [17,31], active faults [1] and historical earthquake epicenters (select data taken from ref. [25]).

The Celje Basin is crossed by by the Savinja River and its tributaries, which deposited a series of terraces during the Pliocene and Quaternary [31]. The pre-Pliocene basement consists of folded Oligocene and Miocene strata [17,18]. The arrangement of Pliocene–Quaternary terraces, with the oldest terraces at the margins and the Savinja River running along the southern margin of the basin, indicates that asymmetric folding continued during the Quaternary and was probably driven by the activity of the Sava–Celje fault [32].

Celeia is located in the Holocene floodplain at the confluence zone between the Savinja and Hudinja rivers in the SE of the basin. The studied site is below the Princes' Palace (Knežji dvor), the 16th century residence of the counts of Celje, now part of the Provincial Museum (Pokrajinski Muzeum, Trg celjskih knezov 8). The building is located less than 100 m north of the Savinja River and 700 m west of the Hudinja River, in a flat terrain about 200 m north of the southern slopes of the basin, within the fault zone of the Celje fault (Figure 2). The groundwater is therefore very shallow below the surface, according to the nearest hydrogeological boreholes only 2–3 m below the surface [33]. (However, archaeologists excavating down to a 3.8 to 4 m depth have never seen groundwater.) The thickness of the Quaternary deposits near the site is only 5–8 m; these consist mainly of sandy to silty gravel with individual silt and sand layers between the gravel [33,34], while sands predominate closer to the Hudinja River [35].

1.2. Celeia History and Structure

Celeia, a town of merchants and craftsmen, had flourished since ancient times. Its population was of Celtic origin. Romanization started early, even before the annexation to the Empire in 15 BC. In Claudian times (AD 41–54) it became a town of Noricum province, extending on the northern bank of the River Savinja, surrounded by its tributaries. Pliny lists its name in his *Naturalis Historia*; therefore, it had become an important administrative centre in Noricum province by that time. Abundant inscriptions found throughout the centuries in secondary positions inform us about the inhabitants of the *municipium*. In situ archaeological finds are rare—the lowest archaeological objects remaining from Roman Celeia are up to 7 m below the level of modern Celje. Excavations proved that Celeia was designed according to Roman urban planning rules. The WNW–ESE-trending main street, the *decumanus maximus*, was crossed by at least three NNE–SSE-trending perpendicular streets; the main one was the *cardo maximus*. Pavements of these streets and foundations and floors of public and private buildings were identified during rescue excavations by archaeologists. Additionally, there are numerous walls higher than 2 m (Figure 3) [36].

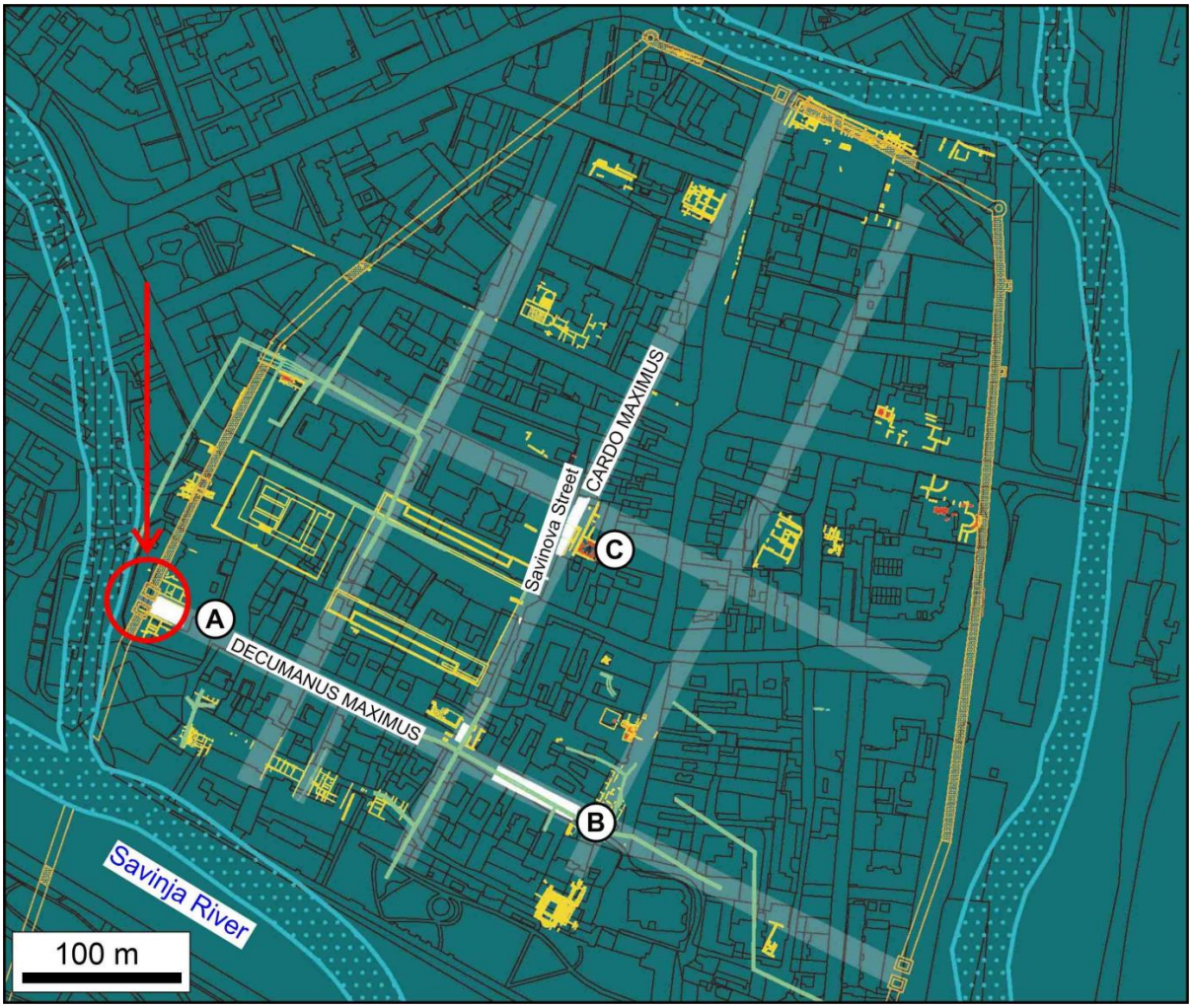

Figure 3. Excavated Roman ruins below the modern streets and houses of Celje (redrawn after ref. [36], modified). (**A**) Roman road, deformed, at the western end of the *decumanus maximus*. Red circle marks the location of the western gate of Celeia. (**B**) Roman road, deformed and repaired by landfill, nearby Forum in the centre along the *decumanus maximus*. (**C**) Roman road, undeformed, along the *cardo maximus*. Locations of photos on Figures 5 to 8 are within the white rectangle enclosed by the red circle.

The rich town's development was halted by the Marcomannic war, which lasted until 182 AD. Recovering from extensive damage, the town was reduced in dimensions, while maintaining a rich architectural program, starting in Severan times (193–211 AD). Unusually, the new structures were built on top of a metre-thick deposit of gravel, considered as flood deposit of the River Savinja or artificial landfill by the Romans. The economic success of the town is marked by the large amount of marble-clad buildings and a marble-paved forum. The main streets (*decumanus maximus* and *cardo maximus*) were raised to a higher level and paved with limestone slabs. The completely renovated town prospered into the fourth century, decorated with porticoed streets and a large, richly decorated forum. In the middle of the fourth century, Celeia was enclosed by a monumental masonry wall, built probably during the reign of Emperor Constans (337–350 AD). The once affluent town declined by the sixth century, mostly due to Barbarian incursions. While town life did not cease after this period, the lack of major construction work resulted in the Late Antique ground level being almost the same level as the Medieval ground.

We carried out an archaeoseismological study of an in situ preserved part of a Roman road in Celje, which shows various anomalies compared with regular roads of that time.

1.3. A Roman Road—Construction Methods

Roman roads in affluent towns were built with bedding (*rudus*) of rammed-down layers of stone rubble and gravel. Main roads were paved with flat limestone slabs (Figure 4). The main east–west road in Celeia, the *decumanus maximus* had a 6 m wide paved surface, gently inclined from the centre to both sides, to allow rainfall to rapidly reach the stone-paved canals on both sides. Adjoining sidewalks, up to 4 m wide, paved or unpaved, followed the road [36].

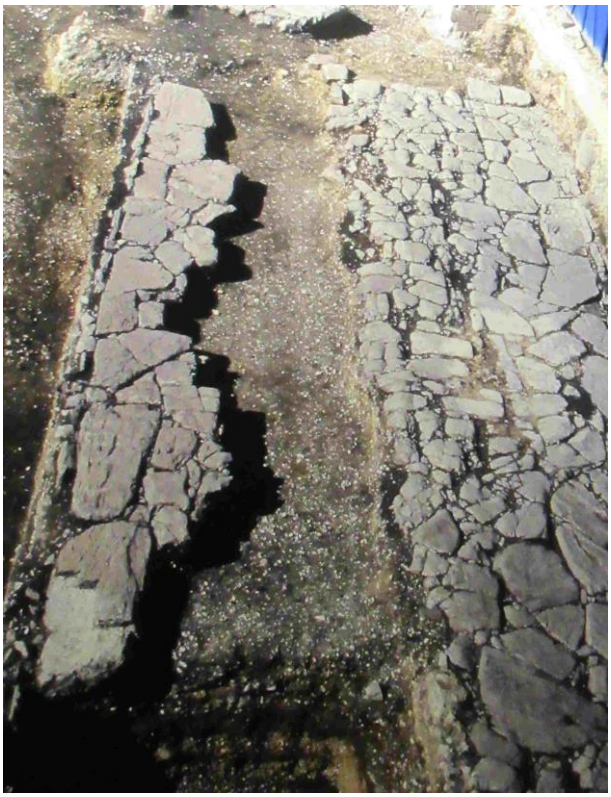

Figure 4. Undeformed Roman road: a 37 m long section of the *cardo maximus,* as discovered in Savinova ulica, excavation in 1989 (redrawn after ref. [36], modified), p. 61. ADB photo #dia_1978, from the Pokrajinski Muzej, Celje.

2. Materials and Methods

The Celje Regional Museum, located in the Princes' Palace (Trg Celjskih knezov 8), has an underground exhibition hall, *Mesto pod mestom* (=Town beneath town), built over the in situ Roman road and parts of the west gate of Celeia. The floor level of the hall and of the road is 3.0 m below the entrance to the palace building. An in situ portion of the road is exhibited. The road and the remaining walls of the west gate were studied in detail, documenting deformation features that can be attributed to seismic events [37,38]. The photographic structure-from-motion technique was applied to provide views which would be otherwise inaccessible and invisible in the tight underground space of the exhibit. Documentation included taking 700 photos with a Canon PowerShot SX620 HS camera. 3D photographic models were built with the Agisoft Metashape software for visualization purposes [39]. The models are provided as Supplementary Models S1–S3. Horizontal and vertical dimensions were measured by a Leica Disto 8 laser range finder. The potential seismic intensity was assessed based on combined use of the earthquake archaeological effect (EAE-13) scale [40], referring damage in archaeological settings to the EMS98 scale [30] and the Environmental Seismic Intensity Scale 2007—ESI 2007 [41].

3. Results

The deformed road as exhibited in situ in the underground museum hall features a pavement made of irregular slabs, separated by gaps several centimetres wide (Figure 5). A reconstructed original cross-section of the *decumanus maximus* is drawn on the eastern wall of the museum hall. Opposed to the flat surface of the road as shown in the reconstruction, the surface on display shows significant differences: it has two convex features, different in size, a concave feature between them, and steep margins, tilted towards both flanking ditches. The maximum difference in altitude between the lowest and highest points is 40 cm within the 6 m wide road. Most of the pavement slabs are horizontal or gently tilted, but those on the southern flank (point B on Figure 5) are oriented with a tilt of max. 40° towards the ditch. Those slabs which paved the floor of the ditch, laid horizontally, are now tilted by 20° inwards (Figure 6).

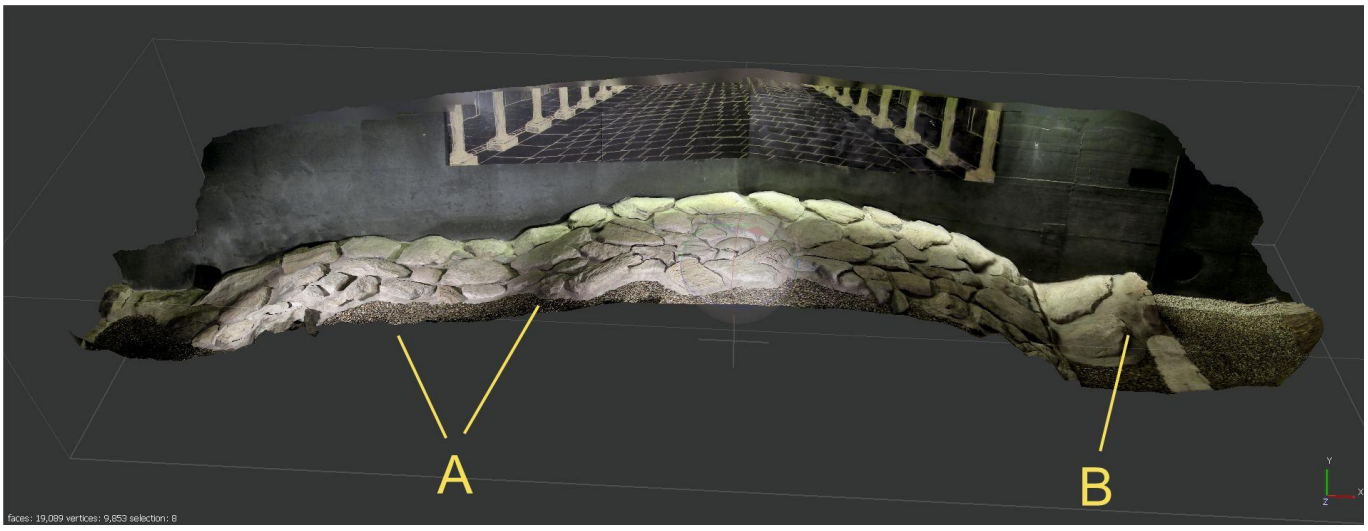

Figure 5. East end of the main Roman road, the *decumanus maximus*, exhibited in situ in the undergound museum Mesto pod mestom in Celje. The road is 6 m wide; with the adjacent paved ditch and sidewalk, it reached 14 m width. The maximum difference in altitude between the lowest and highest points is 40 cm within the 6 m wide road. 3D model by Agisoft Metashape. See the original, flat surface, mildly tilted towards the colonnade, on the graphical reconstruction behind. Deformation features: A—trench-like subsidence. B—pop-up structure of flagstones of the sidewalk (see Figure 6). View to east. For location, see Figure 3.

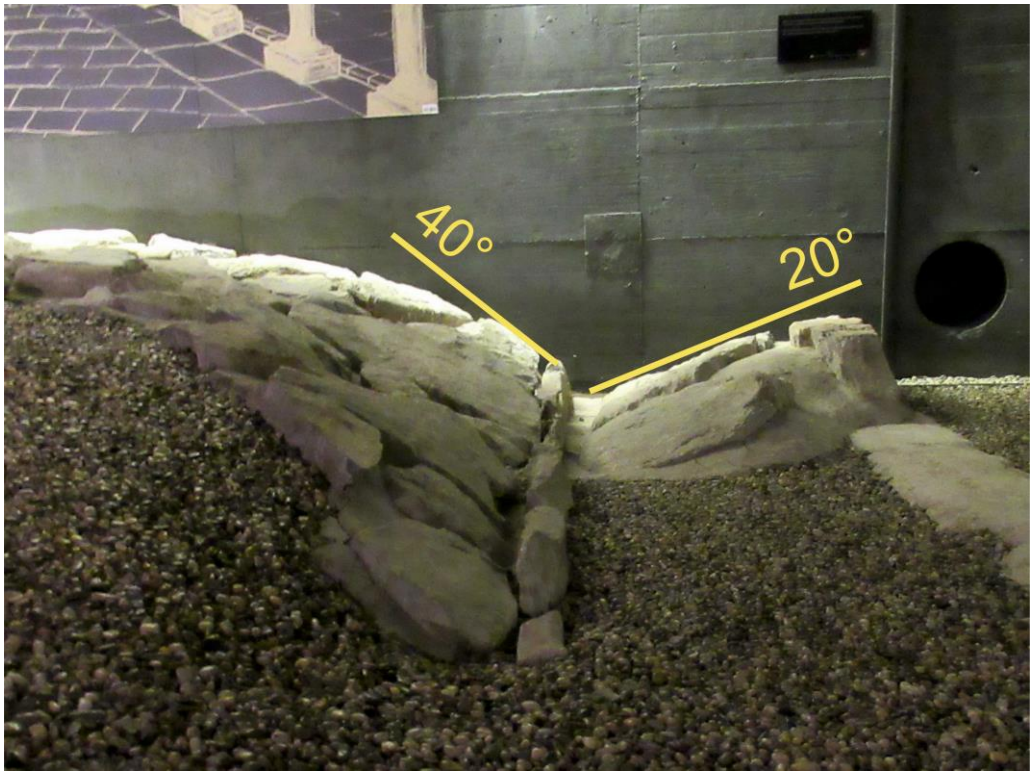

Figure 6. Deformed ditch paved with slabs along the southern edge of the road (location B on Figure 5). Road surface (left) is tilted by 40°. The adjacent flagstone of the horizontal sidewalk is tilted by 20° towards the road surface. Field of view is 1.8 m wide. View to east. Archaeoseismological Database (ADB) photo #4459. For location, see Figure 3.

The western end of the road carries two edifices, parts of the west gate towers of the town. The south tower (Figure 7) was built over the steeply tilted surface of the road. The north tower (Figure 8) was also built on top of the road (not visible in the plane of the photograph). Construction of these two edifices reduced the original 6 m width of the paved road to 4 m only. Two courses of sandstone ashlars form the upright wall of the north tower. The underlying foundation is about 10–15 cm wider. This foundation contains various, beautifully carved, decorative elements of former buildings: the plinth of a column, a pedestal of a statue, a ledge of a colonnade, and a headless torso, each made of marble. There are further "recycled" elements (*spolia*) of former buildings in the foundation of both towers: parts of old tombstones, headless statues of emperors and architectural members from the forum and the town's main temple.

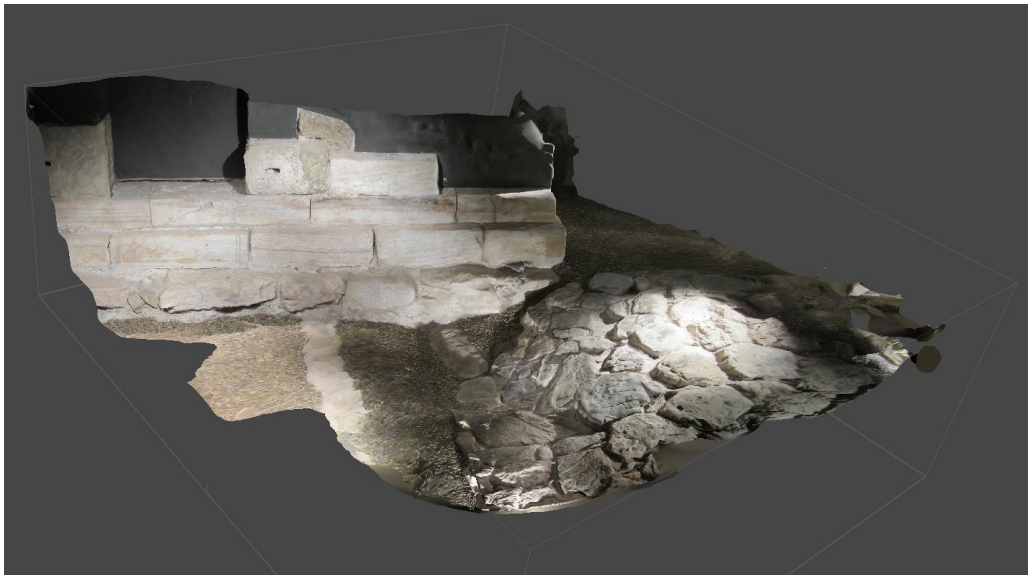

Figure 7. South tower of western gate in the city wall, built on top of the deformed road (location A in Figure 3, encircled). Field of view is ca. 3.5 m wide. View to west. 3D model created by Agisoft MetaShape. For location see Figure 3.

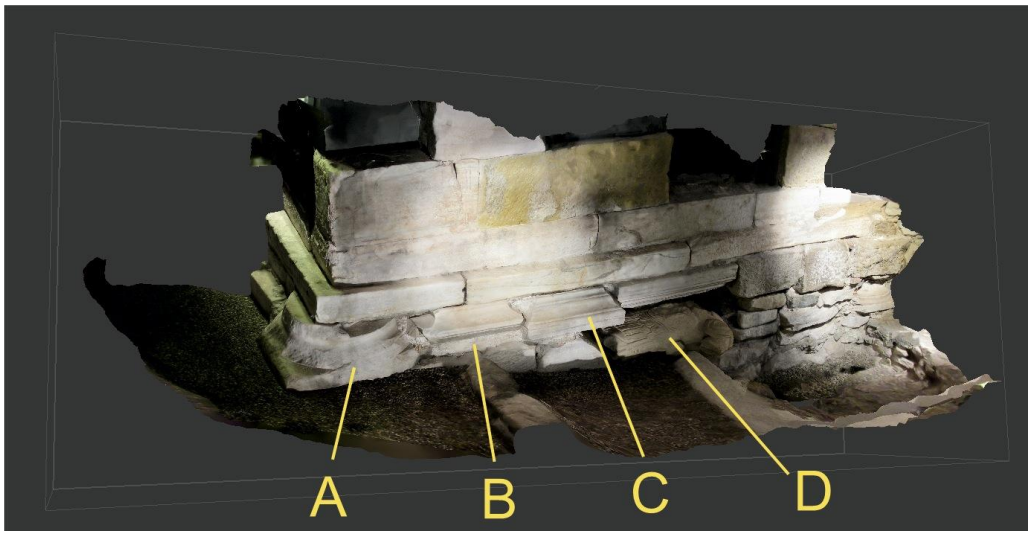

Figure 8. North tower of western gate seen from east, built on top of the deformed road (location A in Figure 3, encircled). Wall built of sandstone ashlars. The foundation (below the 10–15 cm wide ledge) was made of marble *spolia*, i.e., recycled debris of buildings and statues. A—marble plinth of column (left). B—pedestal of a statue. C—ledges from a marble colonnade. D—headless statue of an emperor. Field of view is ca. 4 m wide. View to west–northwest. 3D model created by Agisoft MetaShape. For location see Figure 3.

4. Discussion

4.1. Why an Earthquake?

The deformation features seen on the surface of the exhibited road are interpreted by Bausovac and Krajšek [36] as the result of compaction over a 20 cm deep ditch of an earlier road, lying ca. 1 m deeper, below gravel and sand. While uneven thickness of underlying, compactible material can have an influence on overlying strata, we think that this feature is not sufficient to explain the extensive deformation visible on the road surface.

Earthquake waves, when hitting water-saturated, loose sediments, cause a sudden increase in pore pressure, which in turn increases the distance of grains, in this case of

gravel and sand. The sediment made of disconnected grains loses cohesion, and behaves like a liquid. Structures, such as roads, built on top of the sediment, lose support, suffering deformation in various geometries and ultimately sink into the liquefied sediment. The wavy road surface, showing two "ridges" and a "trough" between them, is the result of the uneven settlement of the heavy stone pavement into the liquefied subsoil. Beyond the differential vertical settlement, the road pavement exhibits horizontal displacement too: the anomalous position of the floor slabs of the ditch, now tilted by 20° inwards, caused the buckling (pop-up structure) of these slabs.

The cross-section of the pavement of Roman roads of this width was traditionally built convex, made of two flat surfaces tilting in opposite directions. Their grades perpendicular to the road axis are usually between 5 and 10%, to help rapid drainage [42]. Five to ten percent are 3° and 6°, respectively, a fraction of the measured 20° to 40° tilt of slabs on the Celeia road.

This kind of liquefaction causing uneven subsidence can be formed on any sediment with saturated pore space, but is more common for sand. The gravel constituting the subsoil below the road is eminently suitable for the purpose. Up to 8 m thick, saturated sandy to silty gravel contains individual silt and sand layers—both above and below an older road level, which were likely the source of liquefaction. There are similar features described and illustrated from a variety of archaeological locations in the seismically active Mediterranean region. A few examples of undulating deformations are in the road-bed of the *central decumanus* at the Greco-Roman site of Tindari, Sicily, associated with a fourth-century earthquake [43]. There is uneven subsidence of a Roman road in Savaria (the Roman Garden, Szombathely, Hungary), caused by seismically induced liquefaction of the subsoil [11]. A seismically induced landslide caused folded and upthrusted remains at the NW corner of the Forum in Roman Baelo Claudia, Spain between AD 40 and 60 [37]. Liquefaction destroyed the port of Messina during the 1908 earthquake, causing metre-scale, differential subsidence [44,45]. Liquefaction-induced deformation was observed on a Roman road in Umm Qais (Gadara), Jordan [46]. There are tilted and folded pavements and stairs of the Propylon in Lagina (Western Anatolia, Turkey) [47].

The sudden availability of valuable *spolia* from major public buildings and statues are an indication that these constructions lost their social role for various reasons, e.g.,: (1) change of religion from the imperial cult to Christianity; (2) *damnatio memoriae* of an emperor or high official; and ultimately, (3) edifices and statues were severely damaged or collapsed in a natural catastrophe, in the case of Celeia, an earthquake. When protective walls had to be built around the town to reduce the chances of enemy attack, it was all the more natural to reuse masonry which was found within city limits, as former parts of destroyed buildings that were not purposed for rebuilding. We suggest the latter case: a severe earthquake damaged the great public buildings of the town, and their components were used to build the defensive walls.

4.2. Estimating the Date

When did the earthquake occur? The slab-paved road was built during the second flourishing period of the town, initiated during the rule of Emperor Severus (193–211 AD). Deformation occurred later, but certainly before the west gate was built, partially blocking the already deformed road. This stratigraphic position offers the key to dating. A coin of Emperor Constans (337–350 AD) was found in the backfill of the foundation trench for the south tower of the west gate. The golden coin was minted in Aquileia between 348 and 350 AD [36], p. 51. This *terminus ante quem* datum, i.e., before which the destruction occurred, is then most probably before 350 AD. We speculate that the interval containing the seismic event is probably the decade before the construction of the defensive wall: this was the main street of Celeia and could not be left unrepaired and useless (as it is now) for the travellers for any period of time. There is an unverified historical datum of a destructive earthquake in 270 AD [48]: whether it was the same or a different event, we cannot tell at the moment. Cecić and Živčić [49] gave a brief note on the supposedly earliest earthquake

on Slovenian territory of 792 AD, expressing doubts that the record is valid. This event is certainly too late for the earthquake damaging the road.

4.3. Intensity and Magnitude

The archaeological intensity scale [40] emphasizes deformation features on upright walls. Out of 17 features only one refers to pavements. Somewhat illogically, there are four pavement deformation features listed among nine off-fault geological effects on the same scale. These can be used to assign intensity to sites where material from walls has been stolen. A major drawback of this scale is that—although it has been widely used since its publication nine years ago, there was neither explanation nor justification published to support the conclusions.

Folds and pop-ups on pavements are ranged into intensity intervals starting at I = VII and extending upwards [40]. The environmental scale (ESI 2007) is also available: major liquefaction, causing >30 cm minimum subsidence between the highest and lowest surface of the deformed road. It yields intensity I = VII–VIII and above [41]. These intensities, being minimum values, do not exclude assigning a higher value to the Celeia event, considering the sudden availability of marble *spolia* stones (see Section 4.1 above). Considering that well-built masonry public buildings were possibly severely damaged and collapsed in the earthquake, we can suggest that the earthquake in question was rather an I = VIII+ (maybe an I = IX) event. However, this higher assignment is to be considered with a low level of confidence.

Usually, the minimum earthquake magnitude value for liquefying sand is estimated to be about 5.5–6 [50,51] (Ambraseys, 1991; Valera et al., 1994), while for gravel-rich deposits about 7 [51] (Valera et al., 1994). Deformed pavements, within the range of amplitude observed in Celeia, are attributed to earthquakes of a similar magnitude range (Table 1).

Table 1. Maximum deformation caused by liquefaction and estimated value of magnitude at selected sites.

Period of Construction	Site	Features	Dimensions	Magnitude	Reference
Roman	Brigetio	Circular depressions	Up to 3 m diameter, 40 cm depth	6.0–6.7 for the destructive 1763 AD event, approx. at the same site	Dobosi and Kázmér (2022) [14] Morais et al. (2017) [52]
Roman	Tindari, Sicily, Italy	Regular, oblique folds on paved road	≤0.43 m amplitude	≤M 6.0 or M 6.1–7.0	Bottari et al. (2008) [43] Barbano et al. (2014) [53]
Modern	Messina, Sicily, Italy	Folded paved road and kerb	<1 m subsidence along the seashore	Mw 7.1	Carcione and Kozák (2008) [44] Pino et al. (2009) [45]

The fault responsible for the earthquake was certainly not far from Celeia. Because portions of the Periadriatic fault system, the Sava fault, the Celje fault, and the Šoštanj fault are all within less than 8 km of the site, any of them could have caused the destruction. Maximum magnitudes were estimated for these faults. For the Sava fault the nearest segment rupture can be as high as M_{max} 6.7; for the total fault rupture estimated M_{max} is 7.1. For the Celje fault M_{max} 6.7 and M_{max} 7.1, respectively; for the Šoštanj fault the individual ruptures of the nearest segments are estimated as M_{max} 5.7–6.7, while the total fault rupture can be as high as M_{max} 7.7. We note that total fault ruptures are unlikely scenarios [1].

Alternatively, estimated magnitudes for the seismic hazard fault model (simplified from the active fault database) are as follow: for the Sava East–Celje seismic source: estimated M_{max} is 7.3, for the Šoštanj West seismic source estimated M_{max} is 7.3 [2]. Maximum magnitudes were estimated for these faults [1,2].

Without assigning responsibility to a single fault, one cannot estimate magnitude. It was certainly much higher than the largest historical earthquake recorded in the immediate vicinity, i.e., the 1974 Mw 4.8, I_{max} VII Kozjansko earthquake [25].

5. Conclusions

The *Mesto pod mestom* museum in Celje exhibits a paved Roman road, part of the west gate of the Roman town of Celeia. The stone pavement suffered severe deformation. Built on fine gravel and sand from the Savinja River, the road displays ridge and trough, pop-up structures, and pavement slabs tilted up to 40°. The city wall was built over the deformed road in Late Roman times, based on a foundation containing recycled material (*spolia*) from public buildings, including an emperor's statue. We hypothesize that a severe earthquake hit the town before 350 AD, causing widespread destruction. Seismic-induced liquefaction caused differential subsidence, deforming the road. The intensity of the earthquake was I = VIII or higher on the EMS98 scale. One of the nearby Sava, Celje, or Šoštanj strike-slip faults was the seismic source of this event. The magnitude was certainly much greater than the largest historical earthquake recorded in the vicinity, the 1974 Mw 4.8, I_{max} VII Kozjansko event.

Supplementary Materials: The following supporting information can be downloaded at: https://www.mdpi.com/article/10.3390/quat6010010/s1, Document S1: Read_me_first; Model S1: Celeia 3D road east end; Model S2: Celeia 3D west gate south tower; Model S3: Celeia 3D west gate north tower.

Author Contributions: Conceptualization, M.K.; methodology, M.K.; writing—original draft preparation, M.K. and P.J.R.; writing—review and editing, M.K., K.G. and P.J.R.; visualization, K.G. and P.J.R.; All authors have read and agreed to the published version of the manuscript.

Funding: P.J.R. acknowledges the support from the ARRS research programme Dynamic Earth (P1-0419). Partial funding was received by K.G. from the Research Excellence Initiative of the University of Silesia in Katowice, Poland.

Data Availability Statement: Not applicable.

Acknowledgments: Maja Bausovac and Jure Krajšek, archaeologists of Pokrajinski Muzej, Celje, were of enormous help in explaining subtle and hidden features of the site. We are also indebted to Ina Cecić for calling our attention to Stopar's historical earthquake data. Academic editors Steven L. Forman and Marcello Tropeano, and four anonymous reviewers made their best efforts to improve the manuscript. We are grateful to all of them.

Conflicts of Interest: The authors declare no conflict of interest.

References

1. Atanackov, J.; Jamšek Rupnik, P.; Jež, J.; Celarc, B.; Novak, M.; Milanič, B.; Markelj, A.; Bavec, M.; Kastelic, V. Database of active faults in Slovenia: Compiling a new active fault database at the junction between the Alps, the Dinarides and the Pannonian Basin tectonic domains. *Front. Earth Sci.* **2021**, *9*, 604388. [CrossRef]
2. Šket Motnikar, B.; Zupančič, P.; Živčič, M.; Atanackov, J.; Jamšek Rupnik, P.; Čarman, M.; Danciu, L.; Gosar, A. The 2021 seismic hazard model for Slovenia (SHMS21): Overview and results. *Bull. Earthq. Eng.* **2022**, *20*, 4865–4894. [CrossRef]
3. Ribarić, V. *Seismicity of Slovenia: Catalogue of Earthquakes (792 A.D.–1981)*; Geoloski Zavod: Ljubljana, Slovenia, 1982; 649p.
4. Nasir, A.; Lenhardt, W.; Hintersberger, E.; Decker, K. Assessing the completeness of historical and instrumental earthquake data in Austria and the surrounding area. *Austrian J. Earth Sci.* **2013**, *106*, 90–102.
5. Kázmér, M.; Győri, E. Millennial record of earthquakes in the Carpathian-Pannonian region—Historical and archeoseismology. *Hung. Hist. Rev.* **2020**, *9*, 281–298.
6. Grützner, C.; Aschenbrenner, S.; Jamšek Rupnik, P.; Reicherter, K.; Saifelislam, N.; Vičič, B.; Vrabec, M.; Welte, J.; Ustaszewski, K. Holocene surface-rupturing earthquakes on the Dinaric Fault System, western Slovenia. *Solid Earth* **2021**, *12*, 2211–2224. [CrossRef]

7. Hinzen, K.-G. Archaeoseismology. In *Encyclopedia of Solid Earth Geophysics*; Gupta, H.K., Ed.; Springer Science: Dordrecht, The Netherlands, 2011; pp. 11–15.
8. Sintubin, M. Archaeoseismology. In *Encyclopedia of Earthquake Engineering*; Beer, M., Patelli, E., Kouigioumtzoglou, I., Au, S.-K., Eds.; Springer: Berlin/Heidelberg, Germany, 2013; pp. 1–17.
9. Kázmér, M. Damage to ancient buildings from earthquakes. In *Encyclopedia of Earthquake Engineering*; Beer, M., Patelli, E., Kouigioumtzoglou, I., Au, S.-K., Eds.; Springer: Berlin/Heidelberg, Germany, 2015; pp. 500–506. [CrossRef]
10. Galadini, F.; Hinzen, K.-G.; Stiros, S. Archaeoseismology: Methodological issues and procedure. *J. Seismol.* **2006**, *10*, 395–414. [CrossRef]
11. Kázmér, M.; Győri, E.; Gaidzik, K. Was Antiquity seismically more active than the Middle Ages?—Roman earthquakes in Pannonia and Dacia. In Proceedings of the 3rd European Conference on Earthquake Engineering & Seismology, Bucharest, Romania, 4–9 September 2022. *submitted*.
12. Ruggieri, N. Seismic vulnerability of the ancient Pompeii through the evaluation of the 62 AD earthquake effects. *Int. J. Archit. Herit.* **2017**, *11*, 490–500. [CrossRef]
13. Konecny, A.; Humer, F.; Decker, K. *(Eds). Das Carnuntiner Erdbeben im Kontext. Akten der III. Internationalen Kolloquiums, 17–18 Oktober 2013*; Archäologischer Park Carnuntum, Neue Forschungen; Amt der NÖ Landesregierung, Abteilung Kunst und Kultur: St. Pölten, Austria, 2019; Volume 14, 159p.
14. Dobosi, L.; Kázmér, M. Late Roman earthquake in Brigetio? In *Pannonia Underground, Proceedings of the International Conference, Szombathely, Hungary, 25–26 November 2021*; Biró, S., Ed.; Savaria Museum: Szombathely, Hungary, 2022; pp. 179–207.
15. Kázmér, M.; Škrgulja, R. The 4th century Siscia (Croatia) earthquake—Archaeoseismological evidence. In Proceedings of the 1st Croatian Conference on Earthquake Engineering, 1CroCEE, Zagreb, Croatia, 22–24 March 2021; pp. 257–266. [CrossRef]
16. Dolenz, H. Ein Erdbeben in der Stadt Alt-Virunum auf dem Magdalensberg? In *Antike Erdbeben im Alpinen und Zirkumalpinen Raum: Befunde und Probleme in Archäologischer, Historischer und Seismologischer Sicht*; Waldherr, G.H., Smolka, A., Eds.; Geographica Historica; Franz Steiner Verlag: Stuttgart, Germany, 2007; Volume 24, pp. 99–115.
17. Buser, S. *Osnovna Geološka Karta SFRJ. L 33-67, Celje*; Zvezni Geološki Zavod: Belgrade, Yugoslavia, 1978.
18. Buser, S. *Tolmač Lista Celje: L 33-67: Socialistična Federativna Republika Jugoslavija, Osnovna Geološka Karta, 1:100,000*; Zvezni Geološki Zavod: Belgrade, Yugoslavia, 1979; 72p.
19. Placer, L. Structural meaning of the Sava folds. *Geologija* **1998**, *41*, 191–221. [CrossRef]
20. Vrabec, M.; Fodor, L. Late Cenozoic tectonics of Slovenia: Structural styles at the north-eastern corner of the Adriatic microplate. In *The Adria Microplate: GPS Geodesy, Tectonics and Hazards*; Pinter, N., Ed.; NATO Science Series IV: Earth and Environmental Sciences; Springer: Berlin/Heidelberg, Germany, 2006; pp. 151–181.
21. Vrabec, M.; Pavlovčič Prešeren, P.; Stopar, B. GPS study (1996–2002) of active deformation along the Periadriatic fault system in northeastern Slovenia: Tectonic model. *Geol. Carpath.* **2006**, *57*, 57–65.
22. Fodor, L.; Jelen, B.; Márton, E.; Skaberne, D.; Čar, J.; Vrabec, M. Miocene-Pliocene tectonic evolution of the Slovenian Periadriatic fault: Implications for Alpine-Carpathian extrusion models. *Tectonics* **1998**, *17*, 690–709. [CrossRef]
23. Jamšek Rupnik, P.; Benedetti, L.; Bavec, M.; Vrabec, M. Geomorphic indicators of Quaternary activity of the Sava fault between Golnik and Preddvor. *RMZ—Mater. Geoenviron.* **2012**, *59*, 299–314.
24. Jamšek Rupnik, P. Geomorphological Evidence of Active Tectonics in the Ljubljana Basin. Doctoral Dissertation, University of Ljubljana, Faculty for Civil and Geodetic Engineering, Ljubljana, Slovenia, 2013; 214p.
25. Živčić, M. *Catalogue of Earthquakes in Slovenia*; Excel Spreadsheet; Internal Documentation; Ministry of Agriculture and Environment, Slovenian Environment Agency, Seismology and Geology Office: Ljubljana, Slovenia, 2009.
26. Hammerl, C. The Earthquake of January 25, 1348: Discussion of Sources. In: EC Project "Review of Historical Seismicity in Europe" (RHISE) 1989–1993. 1994. Available online: https://emidius.mi.ingv.it/RHISE/ii_20ham/ii_20ham.html (accessed on 26 January 2023).
27. Rohr, C. Man and Natural Disaster in the Late Middle Ages: The Earthquake in Carinthia and Northern Italy on 25 January 1348 and its Perception. *Environ. Hist.* **2003**, *9*, 127–149. [CrossRef]
28. Merchel, S.; Mrak, I.; Braucher, R.; Benedetti, L.; Repe, B.; Bourlès, D.; Reitner, J.M. Surface exposure dating of the Veliki vrh rock avalanche in Slovenia associated with the 1348 Earthquake. *Quat. Geochronol.* **2014**, *22*, 33–42. [CrossRef]
29. Stucchi, M.; Rovida, A.; Capera, A.A.G.; Alexandre, P.; Camelbeeck, T.; Demircioglu, M.B.; Gasperini, P.; Kouskouna, V.; Musson, R.M.W.; Radulian, M.; et al. The SHARE European Earthquake Catalogue (SHEEC) 1000–1899. *J. Seismol.* **2013**, *17*, 523–544. [CrossRef]
30. Grünthal, G.; Wahlström, R. The European—Mediterranean Earthquake Catalogue (EMEC) for the last millennium. *J. Seismol.* **2012**, *16*, 535–570. [CrossRef]
31. Mencin Gale, E.; Jamšek Rupnik, P.; Trajanova, M.; Gale, L.; Bavec, M.; Anselmetti, F.S.; Šmuc, A. Provenance and morphostratigraphy of the Pliocene-Quaternary sediments in the Celje and Drava-Ptuj Basins (eastern Slovenia). *Geologija* **2019**, *62*, 189–218. [CrossRef]
32. Mencin Gale, E. Pliocene to Quaternary Sedimentary Evolution of Intramountain Basins at the Junction of Alps, Dinarides and Pannonian Basin. Ph.D. Thesis, University of Ljubljana, Faculty of Natural Sciences and Engineering, Ljubljana, Slovenia, 2021; 187p.

33. Lapanje, A.; Matoz, T.; Janža, M.; Božović, M. *Hidrogeološke Osnove za Zajem Vode za Toplotno Črpalko za Zdravstveni Center Glazija v Celju*; Geološki Zavod Slovenije: Ljubljana, Slovenia, 2009.
34. Drobne, F.; Petauer, D.; Venturini, S. *Poročilo o Geoloških Preiskavah za JEZ-I in JEZ-II na Reki Savinji v Celju*; Geološki Zavod: Ljubljana, Slovenia, 1982.
35. Venturini, S.; Šivec, S.; Peček, D.; Trebec, J.; Vavpotič, K. *Geotehnično Poročilo o Pogojih Temeljenja Objekta za Bivanje in Počitek ob Železniški Postaji v Celju*; Geološki Zavod: Ljubljana, Slovenia, 1982.
36. Bausovac, M.; Krajšek, J. *Municipum Claudium Celeia*; Celeia Antiqua 2; The Celje Regional Museum: Celje, Slovenia, 2020; 120p.
37. Rodríguez-Pascua, M.A.; Pérez-López, R.; Giner-Robles, J.L.; Silva, P.G.; GarduñoMonroy, V.H.; Reicherter, K. A comprehensive classification of Earthquake Archaeological Effects (EAE) in archaeoseismology: Application to ancient remains of Roman and Mesoamerican cultures. *Quat. Int.* **2011**, *242*, 20–30. [CrossRef]
38. Rodríguez-Pascua, M.; Silva, P.G.; Giner-Robles, J.L.; Pérez-López, R.; Perucha, M.A.; Martín-González, F. Arqueosismología: Una nova herramienta para la sismología y la protección del patrimonio. *Rev. Otarq* **2016**, *1*, 151–169. [CrossRef]
39. Forlin, P.; Valente, R.; Kázmér, M. Assessing earthquake effects on archaeological sites using photogrammetry and 3D model analysis. *Digit. Appl. Archaeol. Cult. Herit.* **2017**, *9*, e00073. [CrossRef]
40. Rodríguez-Pascua, M.; Silva, P.G.; Pérez-López, R.; Giner-Robles, J.-L.; Martín-González, F.; Perucha, M.A. Preliminary intensity correlation between macroseismic scales (ESI07 and EMS98) and Earthquake Archaeological Effects (EAEs). In *Seismic Hazard, Critical Facilities and Slow Active Faults, Proceedings of the 4th International INQUA Meeting on Paleoseismology, Active Tectonics and Archaeoseismology (PATA), Aachen, Germany, 9–14 October 2013*; Grützner, C., Rudersdorf, A., Pérez-López, R., Reicherter, K., Eds.; PATA Days: Aachen, Germany, 2013; pp. 221–224.
41. Michetti, A.M.; Esposito, E.; Guerrieri, L.; Porfido, S.; Serva, L.; Tatevossian, R.; Vittori, E.; Audemard, F.; Azuma, T.; Clague, J.; et al. *Environmental Seismic Intensity Scale 2007—ESI 2007*; Memorie Descrittive della Carta Geologica d'Italia; Servizio Geologico d'Italia: Rome, Italy, 2007; Volume LXXIV, pp. 7–54.
42. Xeidakis, G.S.; Varagouli, E.G. Design and construction of Roman road: The Case of Via Egnatia in the Aegean Thrace, Northern Greece. In *Environmental and Engineering Geoscience III(1)*; Spring: Berlin/Heidelberg, Germany, 1997; pp. 123–132.
43. Bottari, C.; Carveni, P.; Sacca, C.; Spigo, U.; Teramo, A. Evidence of seismic deformation of the paved floor of the decumanus at Tindari (NE, Sicily). *Geophys. J. Int.* **2008**, *174*, 213–222. [CrossRef]
44. Carcione, J.M.; Kozák, J.T. The Messina-Reggio earthquake of December 28, 1908. *Stud. Geophys. Geod.* **2008**, *58*, 661–672. [CrossRef]
45. Pino, N.A.; Piatanesi, A.; Valensise, G.; Boschi, E. The 28 December 1908, Messina Straits earthquake (MW 7.1): A great earthquake through a century of seismology. *Seismol. Res. Lett.* **2009**, *80*, 243–259. [CrossRef]
46. Fandi, M. Effects of large historical earthquakes on archeological structures in Jordan. *Arab. J. Geosci.* **2018**, *11*, 9. [CrossRef]
47. Karabacak, V. Seismic damage in the Lagina sacred area on the Mugla Fault: A key point for the understanding of the obliquely situated faults of western Anatolia. *J. Seismol.* **2016**, *20*, 277–289. [CrossRef]
48. Stopar, I. *Celje*; Iro Motovun: Motovun, Croatia, 1986; 142p.
49. Cecić, I.; Živčić, M. The Oldest Earthquake in the Slovene Catalogue. XXV General Assembly of the European Seismological Commission, Reykjavik, Iceland, September 1996. Available online: https://www.researchgate.net/profile/Ina-Cecic/publication/274291039_The_oldest_earthquake_in_the_Slovene_catalogue (accessed on 26 January 2023).
50. Ambraseys, N.N. Engineering seismology. *Int. J. Earthq. Eng. Struct. Dyn.* **1991**, *17*, 1–105. [CrossRef]
51. Valera, J.E.; Traubenik, M.L.; Egan, J.A.; Kaneshiro, J.Y. A practical perspective on liquefaction of gravels. In *Ground Failures under Seismic Conditions, Proceedings of the Sessions Sponsored by the Geotechnical Engineering Division of the American Society of Civil Engineers in Conjunction with the ASCE National Convention, Atlanta, GA, USA, 9–13 October 1994*; Prakash, S., Dakoulas, P., Eds.; Geotechnical Special Publication; American Society of Civil Engineers: New York, NY, USA, 1994; Volume 44, pp. 241–257.
52. Morais, E.; Vigh, L.G.; Krähling, J. Preliminary estimation of the prbably magnitude of Komárom 1763 earthquake using fragility functions. In Proceedings of the 16th World Conference on Earthquake, 16WCEE 2017, Santiago, Chile, 9–13 January 2017.
53. Barbano, M.S.; Castelli, V.; Pantosti, D.; Pirrotta, C. Integration of historical, archaeoseismic and paleoseismological data for the reconstruction of the early seismic history in Messina Strait (south Italy): The 1st and 4th centuries AD earthquakes. *Ann. Geophys.* **2014**, *57*, S0192.